Supporting Information

H-aggregates Granting Crystallization Induced Emissive Behavior and Ultralong Phosphorescence from a Pure Organic Molecule

Elena Lucenti,[a] Alessandra Forni,[a] Chiara Botta,[b] Lucia Carlucci,[c] Clelia Giannini,[c] Daniele Marinotto,[c] Andrea Previtali,[c] Stefania Righetto[c] and Elena Cariati[c,]*

a) ISTM-CNR, Istituto di Scienze e Tecnologie Molecolari – Consiglio Nazionale delle Ricerche and INSTM UdR, via Golgi 19, 20133 Milano, Italy.,

b) ISMAC-CNR, Istituto per lo Studio delle Macromolecole - Consiglio Nazionale delle Ricerche and INSTM UdR, Via Corti 12, 20133 Milano, Italy.

c) Department of Chemistry, Università degli Studi di Milano and INSTM UdR, via Golgi 19, 20133 Milano, Italy.

Experimental Details

Luminescence measurements. Photoluminescence quantum yields were measured using a C11347 Quantaurus – Absolute Photoluminescence Quantum Yield Spectrometer (Hamamatsu Photonics K.K), equipped with a 150 W Xenon lamp, an integrating sphere and a multichannel detector.
Steady state emission and excitation spectra and photoluminescence lifetimes were obtained using a FLS 980 spectrofluorimeter (Edinburg Instrument Ltd). The steady state measurements were obtained by a 450 W Xenon arc lamp. Photoluminescence lifetime measurements were performed

using: Edinburgh Picosecond Pulsed Diode Laser EPL-375, EPLED-300, (Edinburg Instrument Ltd) and microsecond flash Xe- lamp (60W, 0.1÷100 Hz) with data acquisition devices time correlated single-photon counting (TCSPC) and multi-channel scaling (MCS) methods, respectively.

DFT and TDDFT calculations

DFT and TDDFT calculations on compounds **1** and **2** were performed with Gaussian 09 program (Revision D.01), using the 6-311++G(d,p) basis set. Owing to the observed multi-faceted properties of **1**, a functional able to correctly treat ground and excited states properties, besides dispersive intermolecular interactions, was requested. Several DFT exchange-correlation functionals (PBE0, CAM-B3LYP, B97D and ωB97X) have been tested in order to single out a functional able to properly reproduce in a consistent way the whole set of geometrical, electronic and optical features of the investigated dye **1**, in both monomeric and aggregates forms. On one side, the PBE0 functional was found to accurately reproduce the absorption spectrum of the monomer ($S_0 \rightarrow S_3$ and $S_0 \rightarrow S_4$ transitions computed at 226 nm with f=0.30, close to the experimental λ_{max} value, 220 nm) but failed to provide a stable dimer. The same inability to obtain a convergence dimer was found by using the CAM-B3LYP functional. On the other side, the B97D functional, while providing stable dimers and larger aggregates, was found to be instable for TD calculations. Only the ωB97X functional was shown to provide both acceptable absorption spectra for the monomer ($S_0 \rightarrow S_3$ and $S_0 \rightarrow S_4$ transitions computed at 203 nm with f=0.56) and stable dimer and tetramer aggregates. The same functional was also able to provide a stationary state for the S_1 singlet excited state of both monomer and dimer. Therefore, the latter functional was chosen for all ground and excited states calculations.

In Tables S1 and S2 we report the first singlet and triplet excitation energies for the monomer and the dimer at the respective ground state geometries. The difference between the S_1 and T_1 excitation energies corresponds to the 'vertical' ΔE_{ST} energy gap and provides only a first approximation to the experimentally observed singlet−triplet energy gap, owing to the neglecting of geometry relaxation that could arise in crystal structure. In fact, the computed ΔE_{ST} was significantly larger than the experimental one (1.57 and 1.55 eV for the monomer and the dimer, respectively, to be compared with the observed value of about 0.7 eV). A better approximation should be provided by the 'adiabatic' ΔE_{ST}* energy gap, which differently from ΔE_{ST} takes into account excited-state geometry relaxations due to optimization of both S_1 and T_1 states, which is however hampered by the intrinsic difficulty in optimizing T_1 at the TDDFT level. Besides the neglecting of geometry relaxation, moreover, it should be also taken into account that this data is strongly dependent on the adopted functional, owing to a significant shift of the triplet level with respect to the singlet one, which is instead rather stable with varying the functional. For example, ΔE_{ST} reduces to 1.49 and 1.11 eV for the monomer when using CAM-B3LYP and M06-2X, respectively, on the optimized ωB97X structures.

Calculations were performed on compounds **1** and **2** at the same level of theory, considering in both cases the monomer and the π-π stacked dimer. For **2**, therefore, the simulated dimer does not represent a good model for the true aggregate form because water molecules, which are present in

the crystal structure of **2**, are not included in calculations owing to the complex network of intermolecular interactions that should be taken into account. At molecular level, the two compounds reveal very similar electronic and optical properties, though the electronic energy of **2** is higher (by 5.49 kcal/mol) than that of **1**, accounting for its formation as minority product during the preparation of **1**. The optimized dimeric forms of **1** and **2** are as well very similar, with a separation between centroids of the central six-membered rings slightly shorter in **1** (3.98 Å) with respect to that of **2** (4.31 Å), but equal interaction energy (-10.11 kcal/mol). However, while for **1** the inter-centroids separation was comparable with the X-ray values (3.73 and 3.95 Å, according to the dimer taken into consideration), in the case of **2** it was much shorter than the experimental value (4.65 Å), owing to the lack of water molecules in the simulated system. These results suggest a reduced π-π stacking interaction in the crystal structure of **2** with respect to that predicted for **1**, in agreement with the observed differences in the emissive behavior of the two compounds in crystal phase.

If not otherwise specified, calculations have been performed in vacuo.

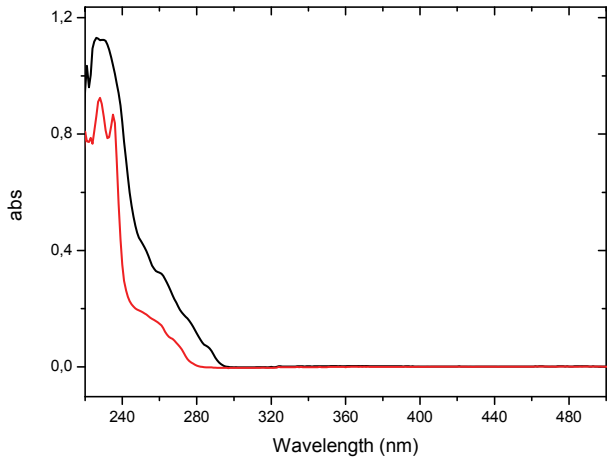

Figure S1 Absorption spectra of **1** and **2** in DCM (2.5×10^{-5}M) at 298 K, black line and red line, respectively.

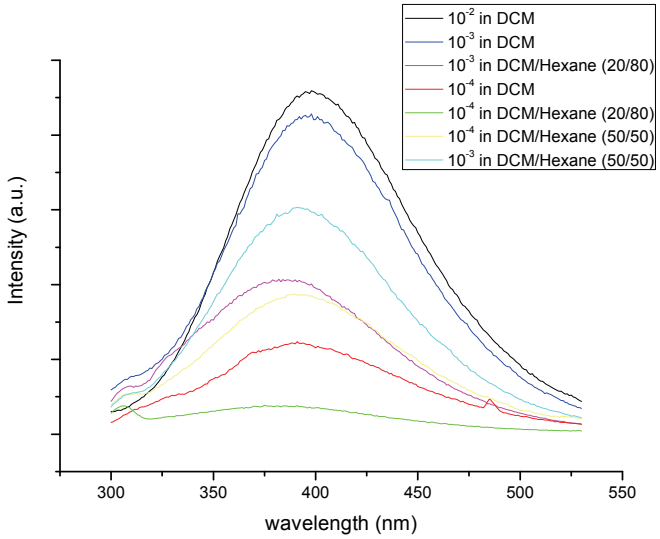

Figure S2 Emission spectra of **1** in DCM-DCM/hexane (different concentrations) at 298 K.

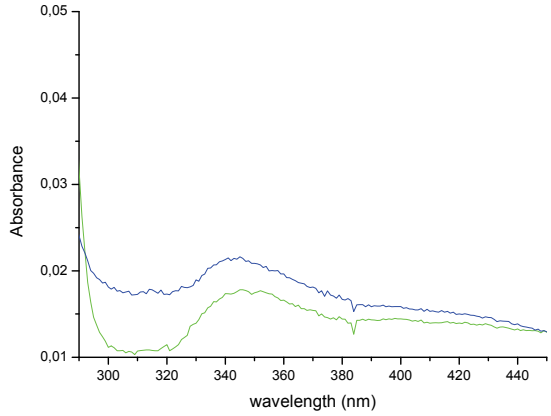

Figure S3 Absorption spectra of **1** in DCM: 10^{-2}M green line, 10^{-3}M blue line.

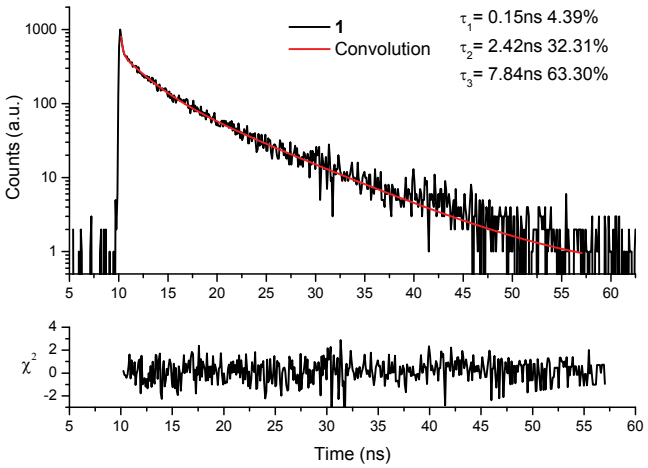

Figure S4a Fluorescence decay of **1** in DCM ($1x10^{-2}$M) at 298 K, black line (λ_{exc} 374 nm; λ_{em} 420 nm) and convolution fit (red line). Weighted residuals (χ^2) are shown under the decay curves.

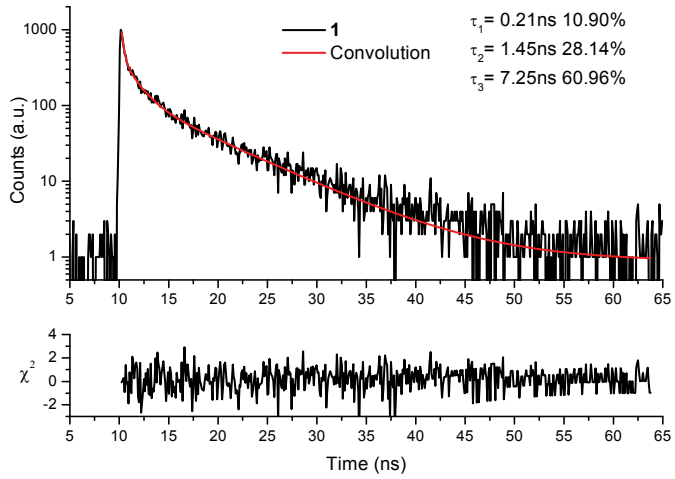

Figure S4b Fluorescence decay of **1** in DCM ($1x10^{-2}$M) at 298 K, black line (λ_{exc} 374 nm; λ_{em} 570 nm) and convolution fit (red line). Weighted residuals (χ^2) are shown under the decay curves.

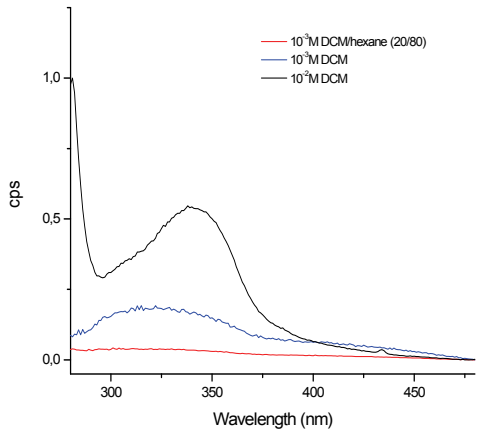

Figure S5 Excitation spectra of **1** in DCM-DCM/hexane at different concentrations (λ_{em} 500 nm)

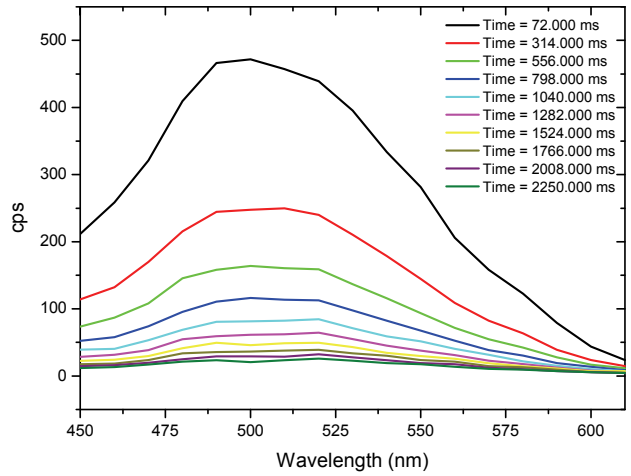

Figure S6a Emission spectra of **1** in DCM ($1x10^{-2}$M) at 77 K recorded at different time delays (λ_{exc}=350 nm).

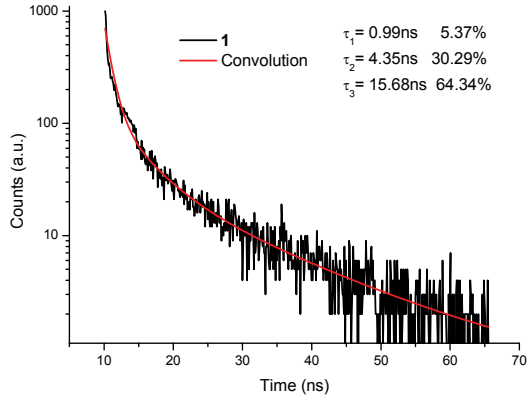

Figure S6b Fluorescence decay of **1** in DCM ($1x10^{-2}$M) at 77 K, black line (λ_{exc} 374 nm; λ_{em} 450 nm) and convolution fit (red line).

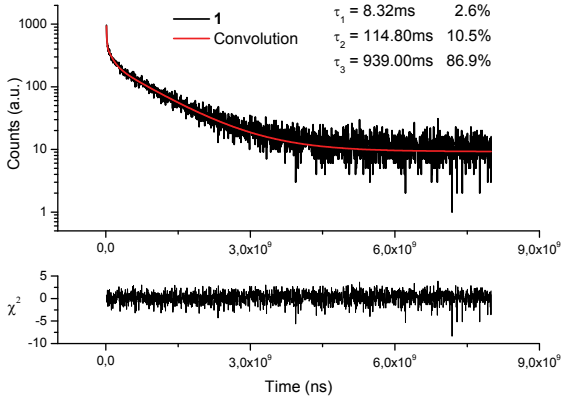

Figure S6c Fluorescence decay of **1** in DCM ($1x10^{-2}$M) at 77 K, black line (λ_{exc} 360 nm; λ_{em} 570 nm) and convolution fit (red line). Weighted residuals (χ^2) are shown under the decay curves.

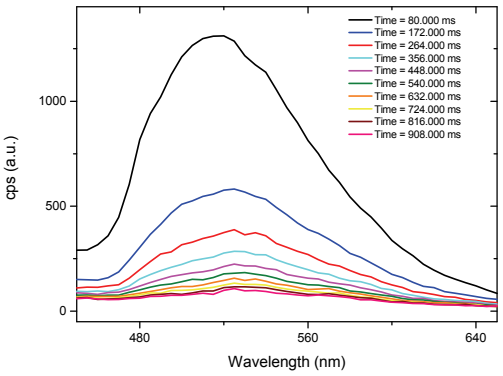

Figure S7 Emission spectra of **1** (powder) at 298 K recorded at different time delays (λ_{exc}=374 nm).

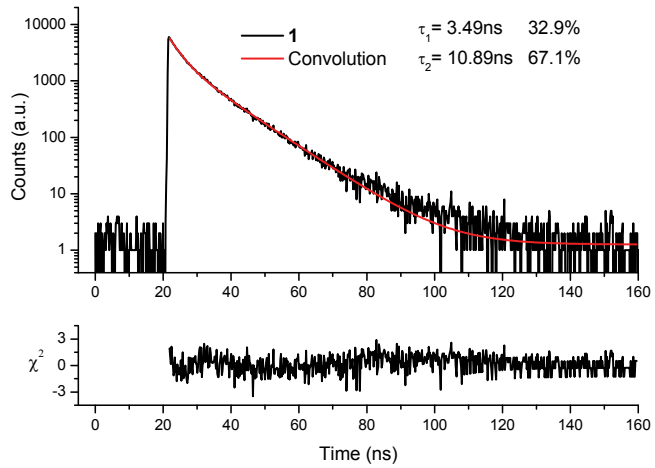

Figure S8a Fluorescence decay of **1** (powder) at 298 K, black line (λ_{exc} 374 nm; λ_{em} 420 nm) and convolution fit (red line). Weighted residuals (χ^2) are shown under the decay curves.

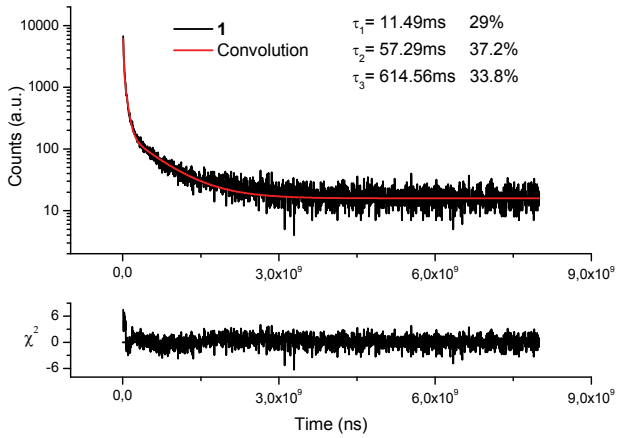

Figure S8b Fluorescence decay of **1** (powder) at 298 K, black line (λ_{exc} 350 nm; λ_{em} 570 nm) and convolution fit (red line). Weighted residuals (χ^2) are shown under the decay curves.

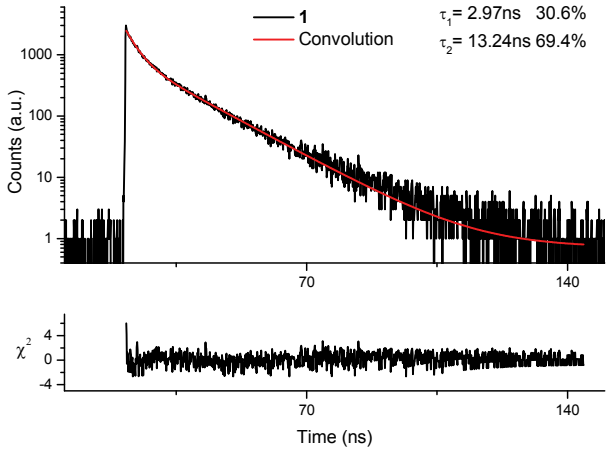

Figure S9a Fluorescence decay of **1** (powder) at 77 K, black line (λ_{exc} 374 nm; λ_{em} 420 nm) and convolution fit (red line). Weighted residuals (χ^2) are shown under the decay curves.

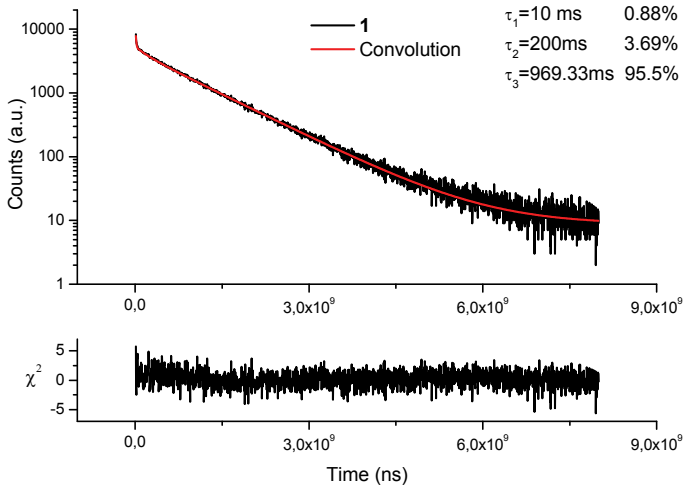

Figure S9b Fluorescence decay of **1** (powder) at 77 K, black line (λ_{exc} 360 nm; λ_{em} 540 nm) and convolution fit (red line). Weighted residuals (χ^2) are shown under the decay curves.

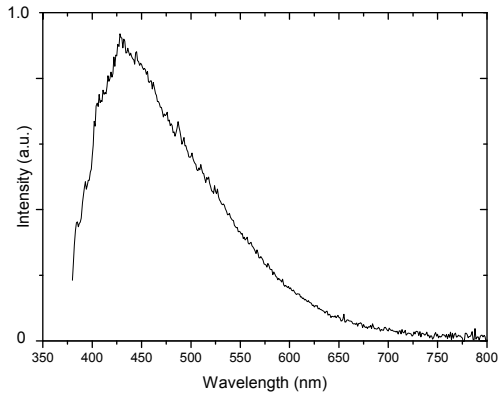

Figure S10a Emission spectrum of **1** (powder) at 77 K, λ_{exc} 360 nm.

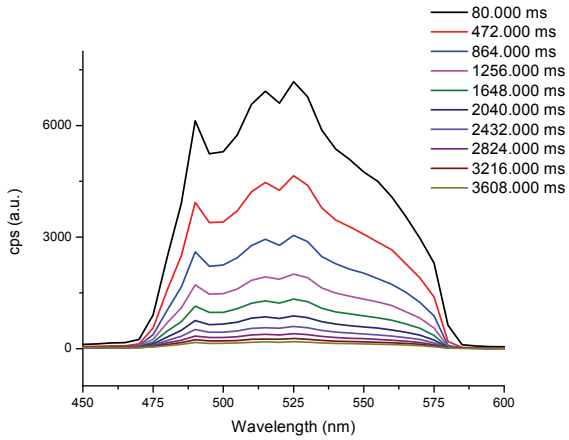

Figure S10b Emission spectra of **1** (powder) at 77 K recorded at different time delays (λ_{exc} = 374 nm)

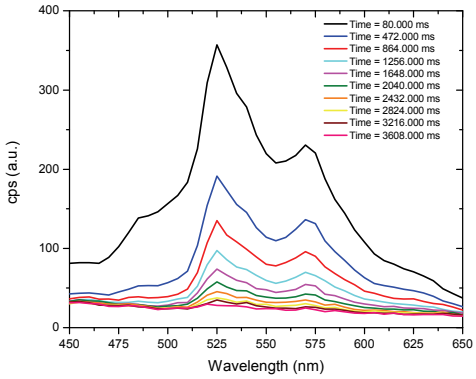

Figure S11 Emission spectra of **1** (crystals) at 298 K recorded at different time delays (λ_{exc}=374 nm)

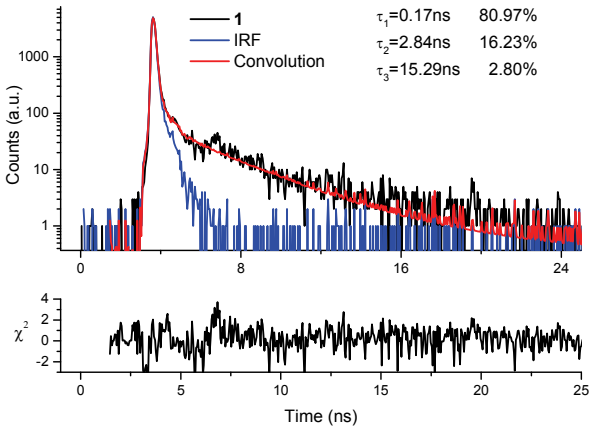

Figure S12a Fluorescence decay of **1** (crystals) at 298 K, black line (λ_{exc} 360 nm; λ_{em} 400 nm) and convolution fit (red line). Weighted residuals (χ^2) are shown under the decay curves.

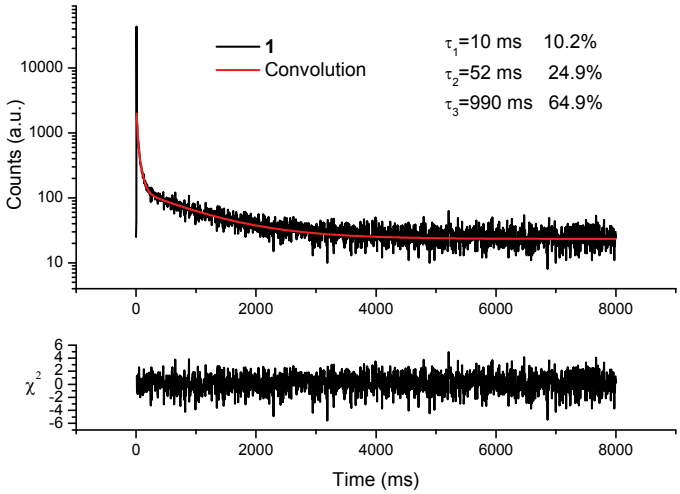

Figure S12b Fluorescence decay of **1** (crystals) at 298 K, black line (λ_{exc} 360 nm; λ_{em} 570 nm) and convolution fit (red line). Weighted residuals (χ^2) are shown under the decay curves.

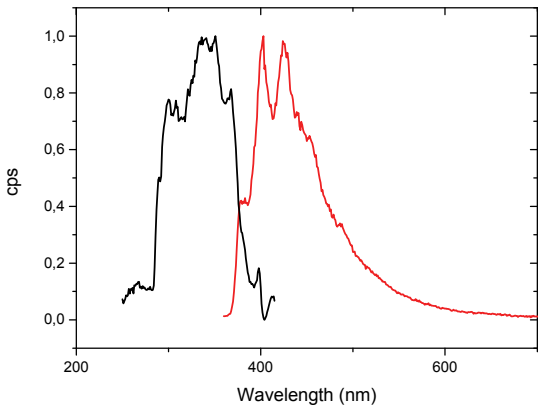

Figure S12c Emission and excitation spectra of **1** (crystals) at 77 K, red and black line respectively.

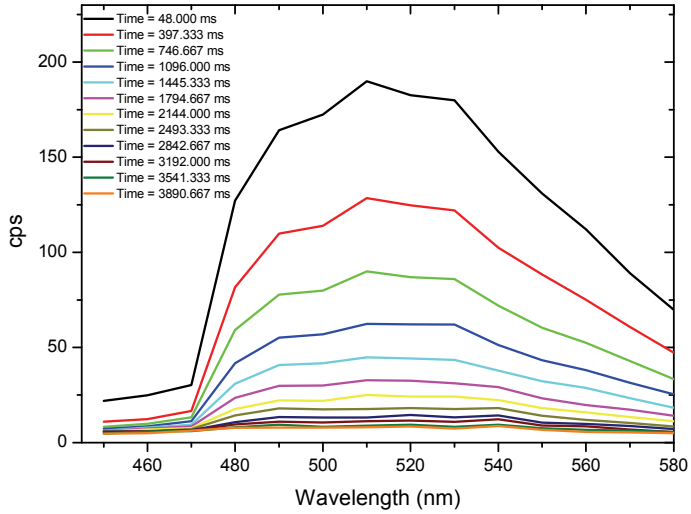

Figure S12d Emission spectra of **1** (crystals) at 77 K recorded at different time delays (λ_{exc}=350 nm).

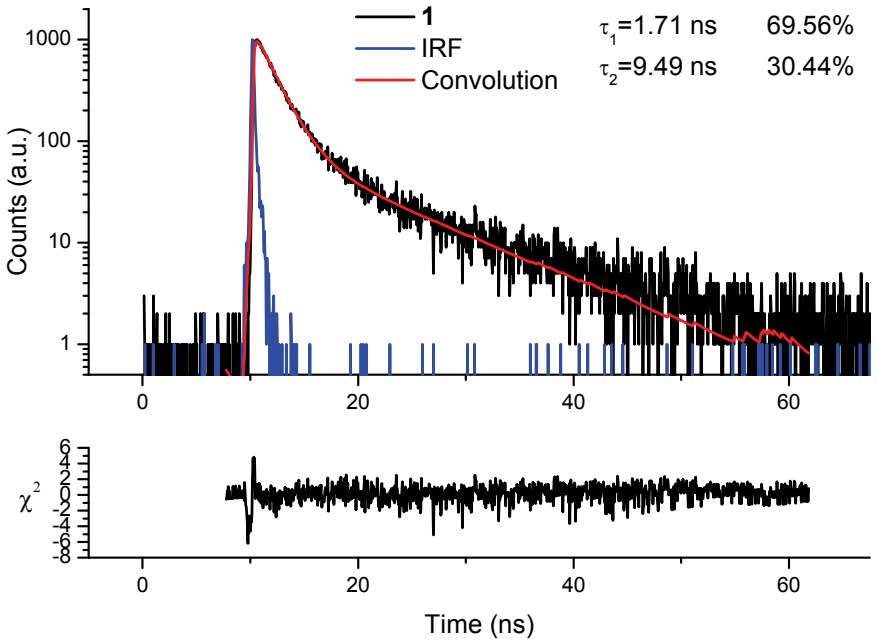

Figure S12e Fluorescence decay of **1** (crystals) at 77 K, black line (λ_{exc} 375 nm; λ_{em} 420 nm), IRF (Instrument Response Function), blue line and convolution fit (red line). Weighted residuals (χ^2) are shown under the decay curves.

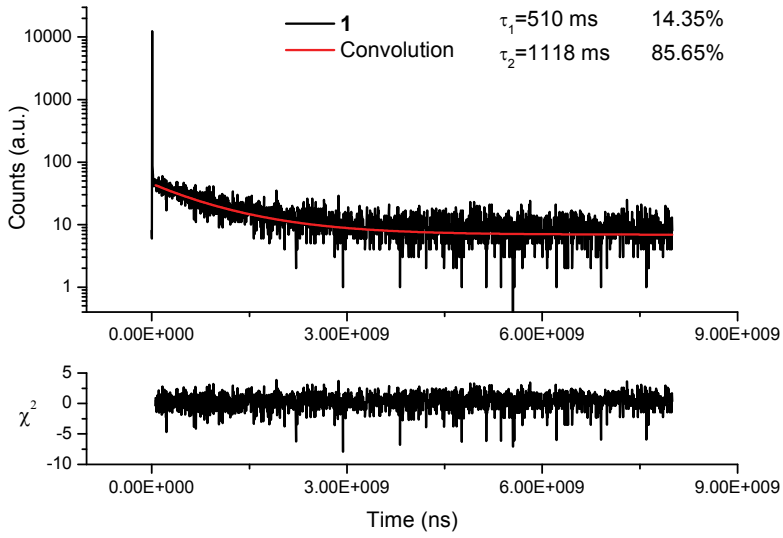

Figure S12f Fluorescence decay of **1** (crystals) at 77 K, black line (λ_{exc} 350 nm; λ_{em} 540 nm) and convolution fit (red line). Weighted residuals (χ^2) are shown under the decay curves.

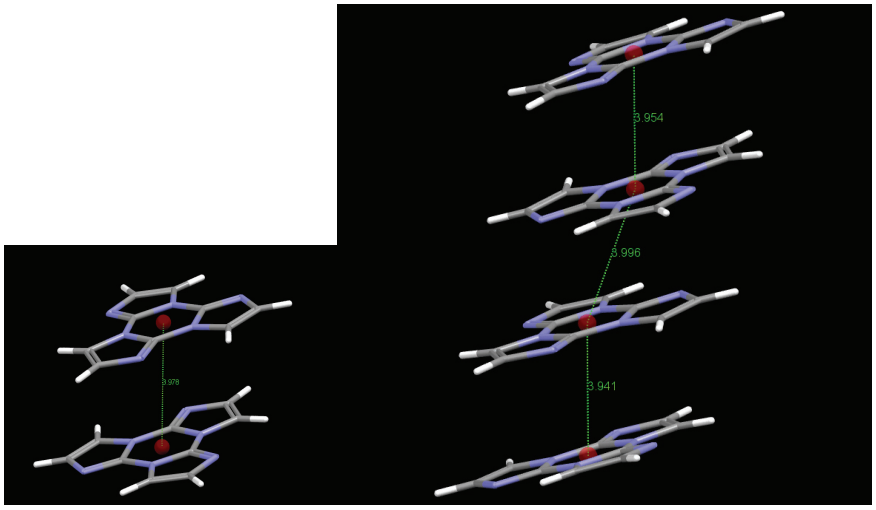

Figure S13 *ω*B97X/6-311++G(d,p) optimized structures of the dimer and tetramer of **1** with distances (in Å) between centroids of the central 6-membered rings.

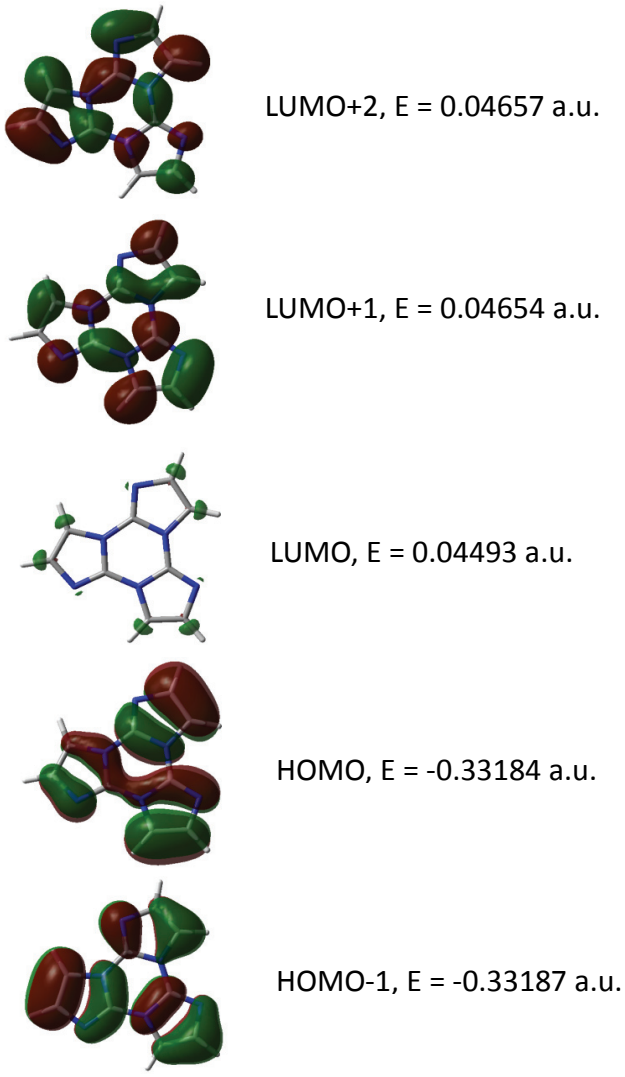

Figure S14a Isodensity surface plot of the frontier orbitals of compound **1** (isosurface values: 0.02, energies in a.u.).

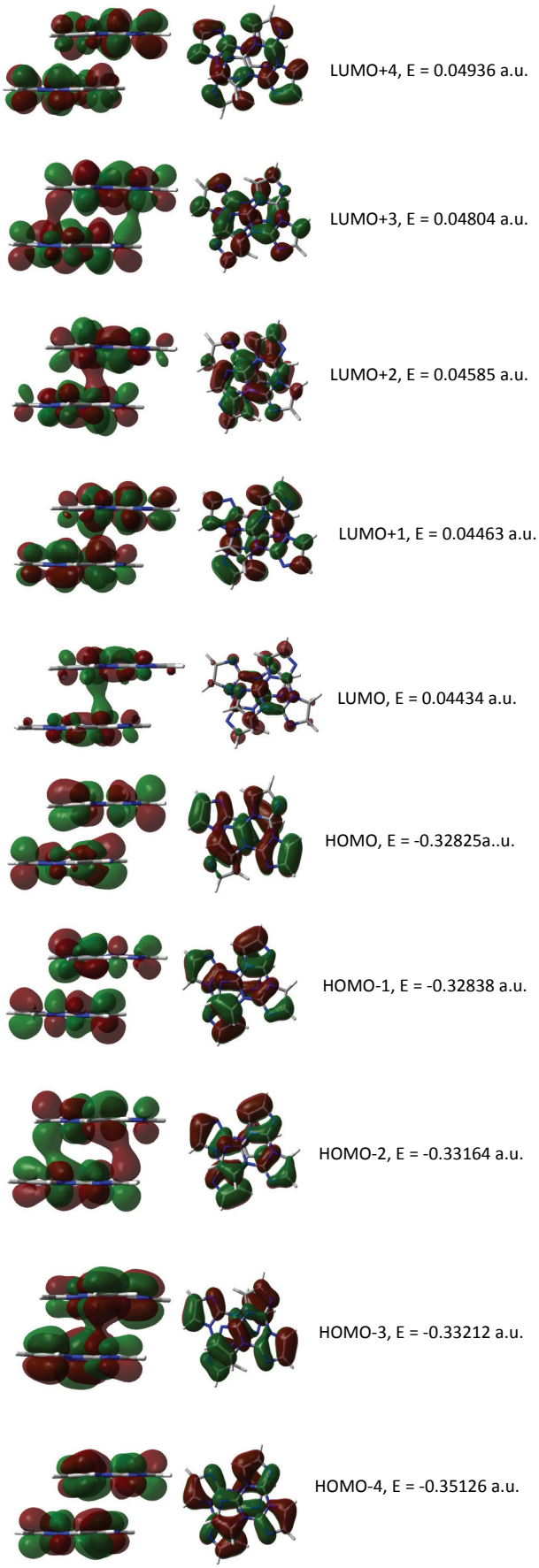

Figure S14b Isodensity surface plot of the frontier orbitals of dimer of compound **1** (isosurface values: 0.02).

Table S1. TD-ωB97X/6-311++G(d,p) $S_0 \rightarrow S_1$ and $S_0 \rightarrow T_n$ (n=1,6) transitions computed on the optimized structure of **1**.

```
Excitation energies and oscillator strengths:

 Excited State   1:      Triplet-A      3.8780 eV  319.72 nm  f=0.0000  <S**2>=2.000
      45 -> 62         0.11041
      50 -> 53         0.21348
      50 -> 54         0.39873
      51 -> 53         0.40157
      51 -> 54        -0.21388

 Excited State   2:      Triplet-A      4.1222 eV  300.77 nm  f=0.0000  <S**2>=2.000
      45 -> 53        -0.11456
      49 -> 53        -0.28646
      49 -> 54         0.20449
      50 -> 53         0.28973
      50 -> 54        -0.18688
      51 -> 53         0.18538
      51 -> 54         0.29034
      51 -> 61         0.14956
      51 -> 62        -0.16955
      51 -> 88        -0.10417

 Excited State   3:      Triplet-A      4.1235 eV  300.68 nm  f=0.0000  <S**2>=2.000
      45 -> 54         0.11443
      49 -> 53         0.20527
      49 -> 54         0.28656
      50 -> 53         0.18683
      50 -> 54         0.29103
      50 -> 61        -0.14991
      50 -> 62         0.16949
      50 -> 88         0.10419
      51 -> 53        -0.28814
      51 -> 54         0.18559

 Excited State   4:      Triplet-A      5.1071 eV  242.77 nm  f=0.0000  <S**2>=2.000
      49 -> 61        -0.13408
      49 -> 62         0.20221
      50 -> 53        -0.38760
      50 -> 54         0.12799
      50 -> 68        -0.11832
      51 -> 53         0.12887
      51 -> 54         0.38994
      51 -> 69        -0.11957

 Excited State   5:      Triplet-A      5.1847 eV  239.13 nm  f=0.0000  <S**2>=2.000
      45 -> 54        -0.12671
      49 -> 53         0.25710
      49 -> 54         0.26449
      49 -> 64         0.10993
      49 -> 69        -0.12645
      50 -> 54        -0.20586
      51 -> 53         0.20489
      51 -> 61        -0.17181
      51 -> 62         0.23138

 Excited State   6:      Triplet-A      5.1853 eV  239.11 nm  f=0.0000  <S**2>=2.000
      45 -> 53         0.12660
      49 -> 53        -0.26496
      49 -> 54         0.25732
      49 -> 63         0.10997
      49 -> 68        -0.12692
      50 -> 53        -0.20662
      50 -> 61        -0.17165
      50 -> 62         0.23132
      51 -> 54        -0.20320

 Excited State   7:      Singlet-A      5.4496 eV  227.51 nm  f=0.0000  <S**2>=0.000
      50 -> 53        -0.36890
      50 -> 54        -0.31584
      51 -> 53        -0.31666
      51 -> 54         0.36915
```

Table S2. TD-ωB97X/6-311++G(d,p) $S_0 \rightarrow S_1$, $S_0 \rightarrow S_1$' and $S_0 \rightarrow T_n$ (n=1,12) transitions computed on the optimized dimeric structure of **1**.

```
Excitation energies and oscillator strengths:

 Excited State   1:      Triplet-A      3.8720 eV  320.21 nm  f=0.0000  <S**2>=2.000
      99 ->106        -0.29152
     100 ->103        -0.12764
     100 ->105         0.17854
     100 ->107        -0.22004
     101 ->104         0.31838
     102 ->105        -0.18964
     102 ->107        -0.22285

 Excited State   2:      Triplet-A      3.8775 eV  319.75 nm  f=0.0000  <S**2>=2.000
      99 ->103        -0.12557
      99 ->105         0.23145
      99 ->107         0.14556
     100 ->104         0.29656
     101 ->105         0.11631
     101 ->107        -0.28027
     102 ->106         0.28831

 Excited State   3:      Triplet-A      4.1072 eV  301.87 nm  f=0.0000  <S**2>=2.000
      97 ->104        -0.15723
      97 ->106        -0.12797
      98 ->107        -0.25458
      99 ->104         0.19096
      99 ->106         0.16082
     100 ->103        -0.11288
     100 ->105         0.17134
     101 ->104         0.16603
     101 ->106        -0.16025
     101 ->121         0.12980
     102 ->105         0.13244
     102 ->107         0.19790

 Excited State   4:      Triplet-A      4.1080 eV  301.81 nm  f=0.0000  <S**2>=2.000
      97 ->107        -0.20500
      98 ->104        -0.24314
      99 ->107         0.23593
     100 ->104        -0.18509
     100 ->121        -0.11406
     101 ->103         0.12895
     101 ->105        -0.19242
     101 ->107         0.10660
     101 ->119         0.11298
     102 ->106         0.21946

 Excited State   5:      Triplet-A      4.1222 eV  300.77 nm  f=0.0000  <S**2>=2.000
      97 ->103        -0.12361
      97 ->105         0.21272
      98 ->104        -0.10808
      98 ->106         0.21706
      99 ->105         0.14429
      99 ->119         0.13221
     100 ->106        -0.25467
     101 ->107         0.19861
     102 ->104        -0.22801
     102 ->106         0.11469
     102 ->121         0.10713

 Excited State   6:      Triplet-A      4.1288 eV  300.29 nm  f=0.0000  <S**2>=2.000
      97 ->104         0.14170
      97 ->106        -0.20127
      98 ->103         0.13072
      98 ->105        -0.21140
      99 ->104         0.14191
      99 ->106        -0.16047
     100 ->105         0.15006
     100 ->107         0.18750
     101 ->104        -0.16493
     101 ->106        -0.14112
     102 ->103         0.11982
     102 ->105        -0.18864
     102 ->107         0.10807
     102 ->119        -0.11409
```

```
Excited State   7:      Triplet-A      5.0701 eV  244.54 nm  f=0.0000  <S**2>=2.000
     97 ->121         0.12730
     98 ->119         0.14040
     99 ->104         0.26498
    100 ->105        -0.12380
    100 ->107        -0.21893
    101 ->106         0.26514
    102 ->103         0.14362
    102 ->105        -0.21129
    102 ->107         0.17105

Excited State   8:      Triplet-A      5.0738 eV  244.36 nm  f=0.0000  <S**2>=2.000
     97 ->119         0.12654
     98 ->121         0.13734
     99 ->103         0.11222
     99 ->105        -0.15551
     99 ->107         0.20307
    100 ->104        -0.11797
    100 ->106        -0.23394
    101 ->103        -0.10601
    101 ->105         0.19360
    101 ->107         0.15537
    102 ->104         0.25436
    102 ->106        -0.13897
    102 ->133        -0.10319

Excited State   9:      Triplet-A      5.1553 eV  240.50 nm  f=0.0000  <S**2>=2.000
     97 ->105         0.15613
     97 ->107         0.14954
     98 ->106         0.26611
     99 ->105        -0.14856
    100 ->106         0.10558
    100 ->118         0.10225
    100 ->121        -0.15540
    101 ->107        -0.16450
    101 ->119         0.17850
    101 ->122        -0.13112
    102 ->104         0.10005

Excited State  10:      Triplet-A      5.1567 eV  240.43 nm  f=0.0000  <S**2>=2.000
     97 ->106         0.21790
     98 ->103        -0.13775
     98 ->105         0.23357
     99 ->106        -0.16639
    100 ->107         0.16125
    100 ->119        -0.13927
    100 ->122         0.10523
    101 ->104        -0.13687
    101 ->118        -0.10846
    101 ->121         0.15244
    101 ->129        -0.11287
    102 ->119        -0.10762

Excited State  11:      Triplet-A      5.1650 eV  240.05 nm  f=0.0000  <S**2>=2.000
     97 ->104         0.23744
     98 ->107         0.23983
     99 ->120        -0.10213
     99 ->121         0.16363
    100 ->105         0.14833
    100 ->127         0.10522
    101 ->106        -0.15662
    102 ->107         0.13738
    102 ->119         0.13643
    102 ->131        -0.10299

Excited State  12:      Triplet-A      5.1684 eV  239.89 nm  f=0.0000  <S**2>=2.000
     97 ->105        -0.12279
     97 ->107         0.20371
     98 ->104         0.24449
     99 ->107         0.12059
     99 ->119         0.15723
     99 ->122        -0.10363
    100 ->104        -0.14698
    101 ->105        -0.12223
    102 ->106         0.14363
    102 ->120        -0.11910
    102 ->121         0.16827
```

```
Excited State  13:      Singlet-A      5.4214 eV  228.70 nm  f=0.0007  <S**2>=0.000
     99 ->104         0.12636
     99 ->106        -0.28745
    100 ->105         0.11535
    100 ->107        -0.28471
    101 ->104         0.30390
    101 ->106         0.12286
    102 ->103         0.16050
    102 ->105        -0.28877
    102 ->107        -0.14076

Excited State  14:      Singlet-A      5.4406 eV  227.89 nm  f=0.0000  <S**2>=0.000
     99 ->103        -0.17051
     99 ->105         0.28684
    100 ->104         0.33394
    101 ->107        -0.32340
    102 ->106         0.32583
```

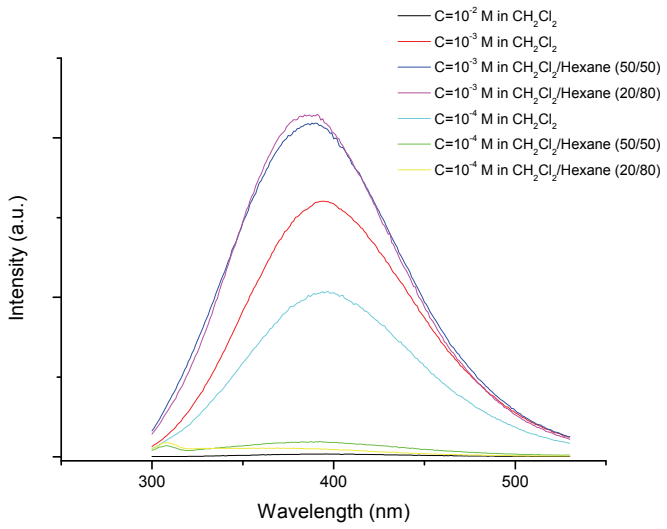

Figure S15a Emission spectra of **2** (DCM and DCM/hexane) at 298 K, λ_{exc}=280nm.

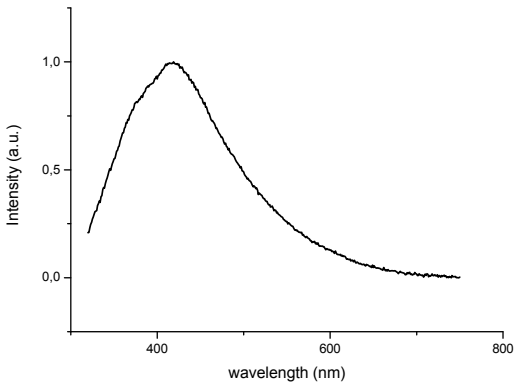

Figure S15b Emission spectrum of **2** (crystals) at 298 K, λ_{exc} 350 nm.

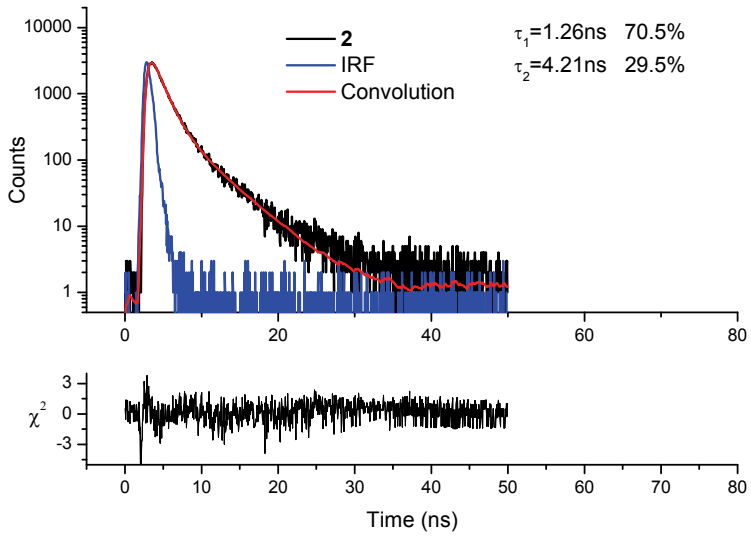

Figure S16a Fluorescence decay of **2** (crystals) at 298 K, black line (λ_{exc} 300 nm; λ_{em} 420 nm) Instrument response function (IRF) and convolution fit blue line and red line respectively. Weighted residuals (χ^2) are shown under the decay curves.

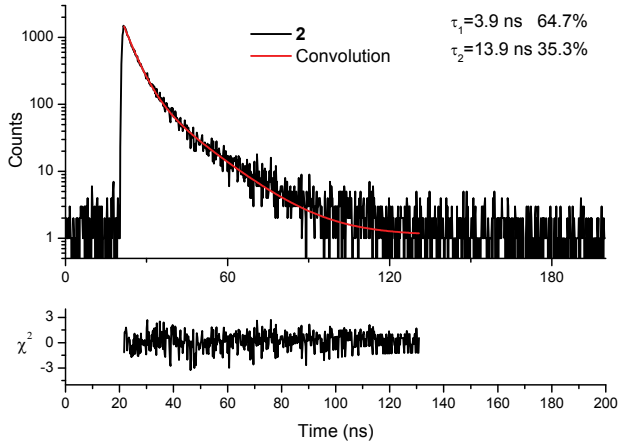

Figure S16b Fluorescence decay of **2** (crystals) at 298 K, black line (λ_{exc} 300 nm; λ_{em} 540 nm) and convolution fit (red line). Weighted residuals (χ^2) are shown under the decay curves.

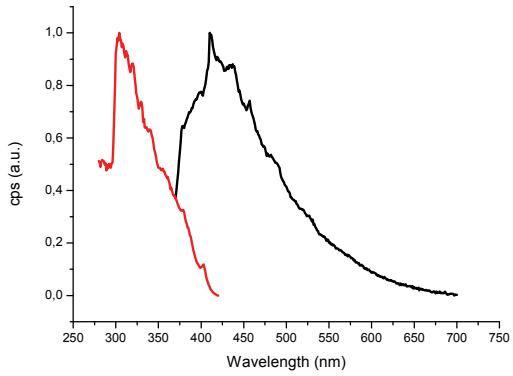

Figure S17 Emission (black) and excitation (red) spectra **2** (crystals) at 77 K, λ_{exc} 350 nm.

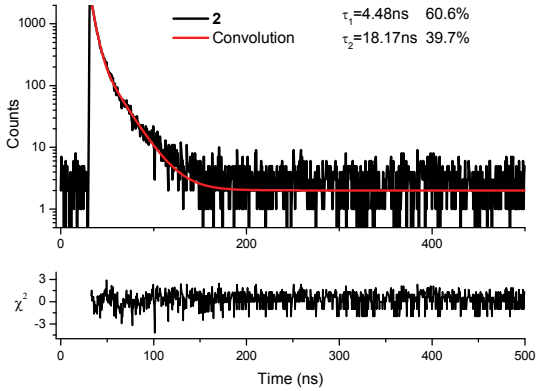

Figure S18a Fluorescence decay of **2** (crystals) at 77 K, black line (λ_{exc} 300 nm; λ_{em} 450 nm) and convolution fit (red line). Weighted residuals (χ^2) are shown under the decay curves.

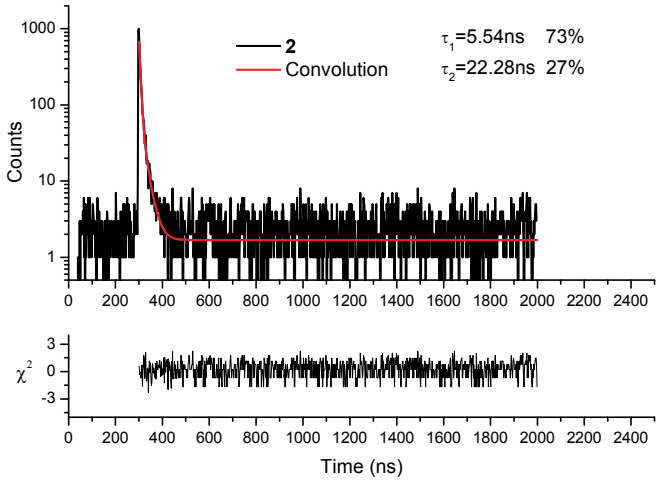

Figure S18b Fluorescence decay of **2** (crystals) at 77 K, black line (λ_{exc} 300 nm; λ_{em} 540 nm) and convolution fit (red line). Weighted residuals (χ^2) are shown under the decay curves.

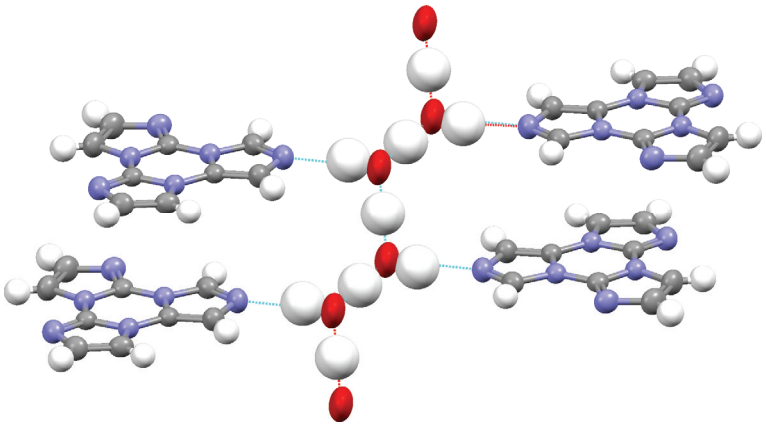

Figure S19. Ortep view down the crystallographic *b* axis showing four stacked molecules of **2** interacting *via* hydrogen bonds with a zig-zag chain of water molecules. Ellipsoids at 50% level of probability.

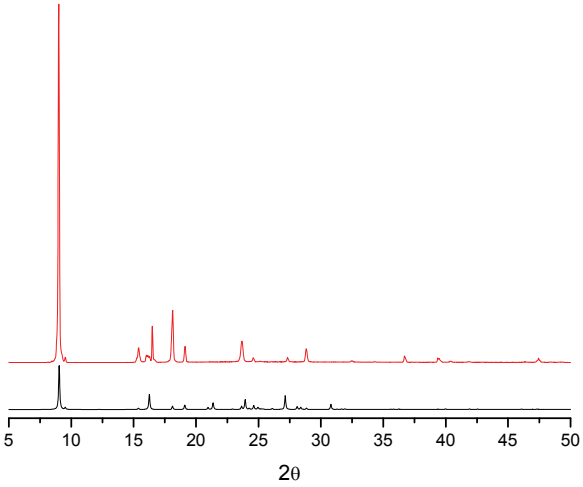

Figure S20 XRPD for compound **2**: Calculated from crystal structure data (black line); experimental collected on gently ground single crystals (red line).

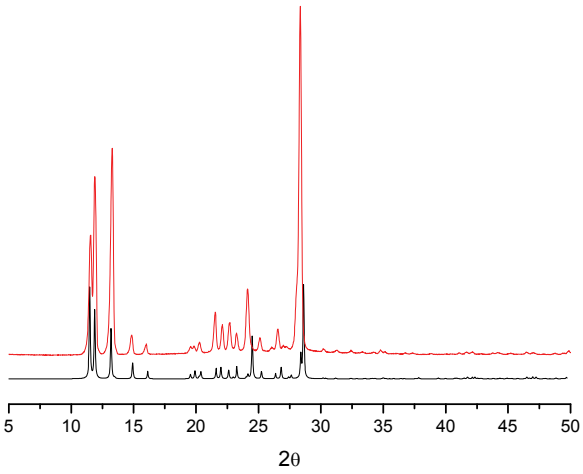

Figure S21 XRPD for compound **1**: Calculated from crystal structure data (Refcode OSEXEQ) (black line); experimental collected on gently ground single crystals (red line).